Nickel diffusion in *B*2-NiGa studied with quasielastic neutron scattering

M. Kaisermayr
Institut für Materialphysik der Universität Wien, Strudlhofgasse 4, A-1090 Wien, Austria

J. Combet
Institut Laue–Langevin, F-38042 Grenoble, France

H. Ipser and H. Schicketanz
Institut für Anorganische Chemie der Universität Wien, Währinger Straße 42, A-1090 Wien, Austria

B. Sepiol
Institut für Materialphysik der Universität Wien, Strudlhofgasse 4, A-1090 Wien, Austria

G. Vogl
Institut für Materialphysik der Universität Wien, Strudlhofgasse 4, A-1090 Wien, Austria
and Hahn-Meitner Institut, D-14109 Berlin, Germany
(Received 15 December 1999)

The weak concentration dependence of Ni diffusivity in NiGa has formerly been interpreted as evidence for Ni diffusion via next-nearest-neighbor jumps, which seems reasonable in the light of the comparably high enthalpy of formation found in this alloy. Quasielastic neutron scattering (QNS) at the backscattering spectrometer IN16 at ILL has been used to study the elementary diffusion jump of Ni in NiGa single crystals near the stoichiometric composition $Ni_{50}Ga_{50}$ as well as in polycrystals with 57 at. % Ni and 62 at. % Ni. While the weak concentration dependence of the Ni diffusion coefficient has been confirmed over a wide concentration range on the Ni-rich site of the NiGa phase diagram, the diffusive jump of Ni atoms unequivocally turned out to be a jump via *nearest-neighbor* sites, i.e., antistructure sites. For the near-stoichiometric compositions it was possible to determine the residence time of the Ni atoms on the antistructure sites *directly* from the QNS measurements. These results indicate very high defect concentrations near the melting temperature.

I. INTRODUCTION

*B*2 structures (also called CsCl structures) consist of two differently occupied sublattices with the sites of the first sublattice being positioned in the center of the unit cell of the second one and vice versa. Hence, in the disordered state the *B*2 lattice becomes a bcc lattice. It is therefore an ''open'' structure, i.e., with few bonds per atom (compared, e.g., to structures of fcc type), and can host a relatively large amount of vacancies.

Despite the simplicity of intermetallic *B*2 structures, diffusion in these technologically promising alloys, which is generally believed to be diffusion via vacancies, is an intriguing subject. This is due to the fact that jumps to nearest-neighbor (NN) sites in these structures are jumps to antistructure sites, hence temporarily disturbing the local order. To overcome this problem several mechanisms like the six-jump cycle, the antistructure bridge mechanism, and the triple-defect mechanism have been proposed, mostly on the basis of the results of tracer diffusion experiments.[1] However, for alloys with high enthalpies of formation, jumps to *next-nearest-neighbor* (NNN) sites which avoid the antistructure site occupation seem more probable.[2]

The diffusion of iron in the *B*2 phase of FeAl which has a comparably low enthalpy of formation has been investigated with quasielastic Mössbauer spectroscopy[3] (QMS) and nuclear resonant scattering[4] (NRS) and has been found to take place via NN jumps. On the other hand, theoretical considerations on *B*2 NiAl, an alloy exhibiting a high enthalpy of formation, indicate that the self-diffusion in this compound is dominated by NNN jumps.[5]

Apparently, the *B*2 phases of NiGa and CoGa find themselves on the borderline between these two regimes, diffusion via NN or NNN jumps (see the enthalpies of formation[6] in Table I). Up to now, no direct information about the diffusive jump in these alloys was available, but conclusions about the self-diffusion mechanism in these alloys have been drawn on the basis of tracer diffusion experiments: Donaldson and Rawlings[7] who investigated the self-diffusion of tracer atoms of both components in NiGa suggested a diffusion mechanism where the nickel atoms diffuse via NNN jumps, i.e., jumps between Ni sites, while the Ga atoms perform NN jumps. Their argument for the NNN jumps of Ni is the concentration independence of the Ni diffusivity which they observed around stoichiometry. This type of jump seems reasonable, taking into account the high enthalpy of formation found in NiGa.[8] Contrary to that, Stolwijk *et al.*[9],

TABLE I. Enthalpy of formation ΔH_f of stoichiometric *B*2 phases exhibiting triple defects taken from Neumann (Ref. 6).

Phase	FeAl	CoGa	NiGa	NiAl
ΔH_f(kJ *g*-atom^{-1})	32.4	36.0	45.0	69.0

who performed detailed tracer diffusion studies on CoGa, a system very similar to NiGa,[10] proposed Co diffusion via antistructure sites, i.e., via NN jumps and Ga diffusion via NNN jumps.

In the present study we investigate *directly* the diffusive jump of Ni in the intermetallic $B2$ alloy NiGa by an atomistic method—quasielastic neutron scattering (QNS). This technique has been successfully applied to study the Ni-diffusion mechanism in the intermetallic $B8$ alloy NiSb (Ref. 11) and the $D0_3$ alloy Ni_3Sb.[12] To our knowledge, the present work is the first application of QNS to self-diffusion in an intermetallic $B2$ structure where diffusion is, in general, slower compared to diffusion in $D0_3$ and $B8$ structures. The study of atoms diffusing at such low rates was enabled by the high-energy resolution and flux of the backscattering spectrometer IN16 at ILL. Preliminary results on one of the samples have been published elsewhere.[13]

II. THEORETICAL MODEL

The diffusive motion of atoms in single crystalline samples leads to a quasielastic broadening of the incoherent scattering function $S(\mathbf{Q},\omega)$ as a function of the momentum transfer $\mathbf{Q}$. For jumps between sites of a Bravais lattice $S(\mathbf{Q},\omega)$ consists of a single Lorentzian with linewidth $\Gamma(\mathbf{Q})$ [full width at half maximum (FWHM)].[14] For NiGa this model applies to NNN jumps where the Ni atoms stay on their sublattice and, therefore, the ''jump lattice'' of the Ni atoms is a simple cubic lattice:

$$\Gamma(\mathbf{Q}) = \frac{\hbar}{3\tau}\sum_{k=1}^{6}\left[1-\exp(-i\mathbf{Q}\cdot\mathbf{l}_k)\right] = \frac{2\hbar}{3\tau}\sum_{i=1}^{3}\left[1-\cos(aQ_i)\right], \tag{1}$$

where a is the lattice parameter and τ the mean residence time on a lattice site. Q_i denotes the ith component of the vector $\mathbf{Q}$. The jump vectors $\mathbf{l}_k$ have the length a and point in a $\langle 100\rangle$ direction (here and in the following, the directions $\bar{1}00$, 010, $0\bar{1}0$, etc., shall be contained in this notation).

For NN jumps the situation is more complicated since two sublattices with different local symmetry are involved. This problem has been treated by Randl *et al.*[15] for general structures and Vogl and Sepiol[3] for the special case of $B2$ structures. The quasielastic spectrum, i.e., the incoherent scattering function $S(\mathbf{Q},\omega)$, is described by the sum of two Lorentzians with $\mathbf{Q}$-dependent linewidths Γ_i and relative weights w_i:

$$S(\mathbf{Q},\omega) = \sum_{i=1}^{2} w_i(\mathbf{Q},\beta)\frac{\Gamma_i(\mathbf{Q},D_{Ni},\beta)/2}{\omega^2+[\Gamma_i(\mathbf{Q},D_{Ni},\beta)/2]^2}, \tag{2}$$

where D_{Ni} is the diffusivity of Ni and β the parameter describing the lattice order (the ratio of the residence times of Ni atoms on the Ga and the Ni sublattice),

$$\beta = \tau_{Ni}^{Ga}/\tau_{Ni}^{Ni} = c_{Ni}^{Ga}/c_{Ni}^{Ni}. \tag{3}$$

Here, c_{Ni}^{Ga} and c_{Ni}^{Ni} are the concentrations of Ni atoms on the Ga and Ni sublattices, respectively. Both the linewidths Γ_i and weights w_i are expressed in terms of the eigenvalues M_i and eigenvectors $\mathbf{b}_i$ of the matrix $\mathbf{A}$ containing the jump vectors $\mathbf{l}_k$ and jump rates τ^{-1} of the diffusing atoms:[3]

$$\mathbf{A} = \begin{pmatrix} -\frac{1}{\tau_{Ni}} & \frac{1}{8\tau_{Ga}}\sum_k \exp(-i\mathbf{Q}\cdot\mathbf{l}_k) \\ \frac{1}{8\tau_{Ni}}\sum_k \exp(-i\mathbf{Q}\cdot\mathbf{l}_k) & -\frac{1}{\tau_{Ga}} \end{pmatrix}. \tag{4}$$

$\mathbf{A}$ has two eigenvalues; hence, $S(\mathbf{Q},\omega)$ is the sum of two Lorentzians with linewidths

$$\Gamma_i(\mathbf{Q}) = -2\hbar M_i(\mathbf{Q}) \tag{5}$$

and relative weights

$$w_i(\mathbf{Q}) = \left|\sum_j \sqrt{c_j}(\mathbf{b}_i(\mathbf{Q}))_j\right|^2. \tag{6}$$

While for smaller $Q(<1\ \text{Å}^{-1})$ the spectrum consists essentially of the narrow Lorentzian, the broad Lorentzian is important at higher Q values where the scattering function is sensible to details on the atomistic scale.

In order to treat correlations of NN jumps we use the following approximation, which will be referred to as the ''effective-jump approximation'': Provided that the residence time of the Ni atom on the antistructure site, τ_{Ni}^{Ga}, is short compared to that on the Ni site, τ_{Ni}^{Ni}, it is possible to replace two consecutive NN jumps by an effective jump in the $\langle 100\rangle$, $\langle 110\rangle$, or $\langle 111\rangle$ direction (Fig. 1). Let $P_{\langle hkl\rangle}$ denote the relative probability for an effective jump in $\langle hkl\rangle$ direction. The linewidth of the quasielastic curve can then be approximated by

$$\Gamma(\mathbf{Q}) = P_{\langle 100\rangle}\Gamma_{\langle 100\rangle}(\mathbf{Q}) + P_{\langle 110\rangle}\Gamma_{\langle 110\rangle}(\mathbf{Q}) + P_{\langle 111\rangle}\Gamma_{\langle 111\rangle}(\mathbf{Q}), \tag{7}$$

where $\Gamma_{\langle hkl\rangle}$ is the linewidth corresponding to an effective $\langle hkl\rangle$ jump in anology to Eq. (1). This approximation allows us to determine the $P_{\langle hkl\rangle}$, which is not possible with the NN-jump model of Eqs. (4)–(6), where the ratio of probabilities for effective jumps is intrinsically that for uncorrelated jumps, $P_{\langle 100\rangle}:P_{\langle 110\rangle}:P_{\langle 111\rangle} = 3:3:1$.

For polycrystalline samples the polycrystalline approximation[14] for isotropic media has to be applied:

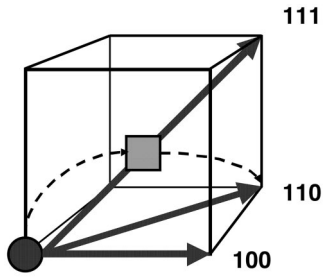

FIG. 1. Unit cell of the $B2$ structure. The corners represent sites of the Ni sublattice, the center a site of the Ga sublattice. The Ga site is occupied by a vacancy (square). The bold arrows symbolize effective jumps of a Ni atom along the $\langle 100\rangle$, $\langle 110\rangle$, and $\langle 111\rangle$ directions. These jumps are a combination of two NN jumps (dashed arrows) with infinite small residence time on the Ga site.

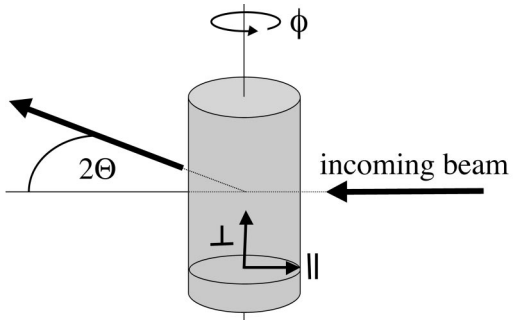

FIG. 2. Schematic representation of the single-crystal orientation. The crystal is first positioned such that the crystal axis $\perp$, which is identical to the geometrical axis of the cylindrical sample, is perpendicular to the scattering plane and that the crystal axis $\parallel$ is parallel to the incoming beam. In a second step the crystal is turned counterclockwise (seen from above) around the angle ϕ in order to obtain different orientations. Hereby, the axis $\perp$ remains perpendicular to the scattering plane while the axis $\parallel$ is no longer parallel to the incoming beam. For the actual values of $\perp$, $\parallel$ and ϕ in the experiment see Table II.

$$\Gamma(Q) = 2\hbar\tau^{-1}\frac{\sin(Ql)}{Ql}, \tag{8}$$

where l is the length of the jump vector.

III. SAMPLE PREPARATION AND ORIENTATION

The measurements near stoichiometry were performed on two cylindrical single crystals, one grown by the Bridgman method and the other one using the Czochralski method. According to microprobe fluorescence analysis the Ni content was 51.2 at. % for the first sample and 52.5 at. % for the second one. The size of the single crystals was 15–20 mm in length and 8–10 mm in diameter.

Due to the NiGa phase diagram,[16] single crystals can only be grown in a small region around stoichiometric composition. This is why we used polycrystalline material for the measurement on the nickel rich side of the phase diagram. The polycrystalline sample had a nickel content of 61.9 at. % and a volume of about 1 cm^3. The grain size was less than 1 mm^3. The corresponding number of grains is expected to be sufficient for averaging when using incoherent scattering where the change of $S(\mathbf{Q},\omega)$ with the momentum transfer $\mathbf{Q}$ is very weak compared to coherent neutron scattering. Another polycrystalline sample with a Ni content of 57.2 at. % consisted of grains that were too large to allow an analysis of the diffusive jump. However, it could still be used to determine the diffusion constant.

The orientation of the single crystals is characterized by the scattering plane including the incoming and the scattered beam and by the direction parallel to the incoming beam (see Fig. 2 and Table II). The single crystal could be turned by an angle ϕ around the rotational axis of the sample which was perpendicular to the scattering plane. The exact macroscopic orientation of the single crystal was measured using the reflection of a laser beam from a polished surface on the top of the crystal. The orientation of the atomic planes in the samples was determined by x-ray diffractometry and turned out to be quite arbitrary (Table II). Nevertheless, we avoided cutting the crystals in order to preserve a cylindrical geometry.

IV. EXPERIMENT

While nickel atoms possess a large incoherent neutron scattering cross section[17] of 5.2 b, the incoherent contribution from the part of gallium is negligible, due to its incoherent cross section of 0.16 b. This allows us to study the motion of nickel atoms without an interfering signal from gallium atoms. Therefore, NiGa is excellently adapted for studying Ni diffusion with neutron scattering.

The measurements were performed at the backscattering spectrometer IN16 at ILL in the unpolished-Si-$\langle 111\rangle$ configuration. This setup provides a Gaussian shaped energy resolution with a width (FWHM) of about 0.9 μeV at a neutron wavelength of 6.27 Å. Six single ^{3}He detectors were installed at scattering angles corresponding to momentum transfers between 0.52 $Å^{-1}$ and 1.89 $Å^{-1}$. The coherent neutron cross sections are 13.3 b for Ni and 6.67 b for Ga, but nevertheless coherent Bragg scattering can be neglected as the first Bragg peak (the $\langle 100\rangle$ superstructure peak) appears at $Q = 2.17$ $Å^{-1}$ which is out of the momentum transfer accessible with the wavelength used in the experiment. According to tracer diffusion measurements[7] the diffusion coefficient of Ni, D_{Ni}, in stoichiometric NiGa near the melting point is of the order of 10^{-12} m^2/s. This corresponds to a quasielastic broadening which is smaller than the width of the resolution function in the setup described above. Therefore special attention had to be paid on the careful measurement of the instrumental resolution function which is folded with the calculated expression for $S(\mathbf{Q},\omega)$ before fitting it into an experimental spectrum. Since even small changes in the experimental geometry can influence the resolution function, we used the samples at room temperature as elastic scatterer to obtain the resolution function. This is justified by the fact that there is no measurable diffusion in NiGa at room temperature. In order to realize the different orientations, the single-crystalline samples which had cylindrical shape were turned around their rotation axes. This allowed us to use the same resolution function for all of the orientations.

TABLE II. Orientation of the single-crystalline samples as defined in Fig. 2.

Sample	T(°C)	Orientations	Crystal axis $\perp$	Crystal axis $\parallel$	Angle ϕ
51.2 at. % Ni	990	1	$\langle 2,\bar{3},\bar{2}\rangle$	$\langle 17,7,7\rangle$	71.8°
51.2 at. % Ni	1060	3	$\langle 2,\bar{3},\bar{2}\rangle$	$\langle 17,7,7\rangle$	71.8°
52.5 at. % Ni	1060	1	$\langle \overline{12},\overline{12},\overline{7}\rangle$	$\langle 12,15,5\rangle$	$-45.0°, 66.7°, -68.5°$
51.2 at. % Ni	1130	3	$\langle 2,\bar{3},\bar{2}\rangle$	$\langle 17,7,7\rangle$	71.8°, 109.8°, 33.8°

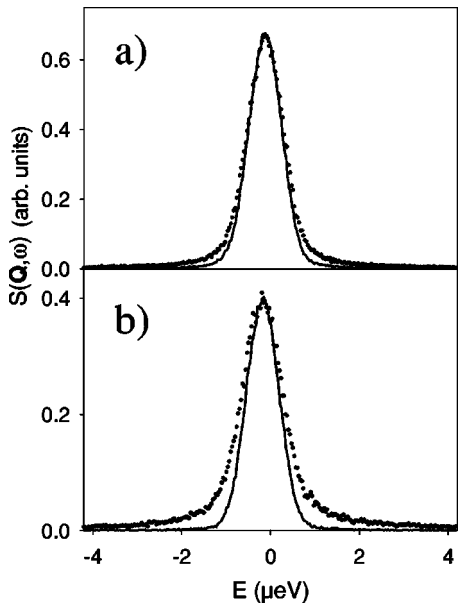

FIG. 3. Quasielastic scattering function $S(\mathbf{Q},\omega)$ in arbitrary units for $Ni_{51.2}Ga_{48.8}$ at 1130 °C at $\mathbf{Q}=0.52$ Å^{-1} (a) and $\mathbf{Q}=1.60$ Å^{-1} (b). The resolution function (solid line) is scaled to the maximum of $S(\mathbf{Q},\omega)$. Counting time: 22 h.

The samples were mounted in niobium sample holders. To avoid contact melting of NiGa with niobium, they where separated by Al_2O_3 ceramics. The Debye-Scherrer ring from Al_2O_3 at 1.8 Å^{-1} was suppressed by covering one of the analyzer mirrors with a cadmium foil. The niobium furnace used in the experiment was supplied by the ILL. Quasielastic spectra were taken at 990, 1060, and 1130°C in one, four, and three different orientations, respectively (see Table II), for the single crystal and at 1040 and 1150 °C for the polycrystalline sample. Figure 3 shows two spectra recorded at two different $\mathbf{Q}$ values on a NiGa single crystal at 1130 °C. These two spectra were taken at the same orientation of the crystal, but at two different scattering angles 2Θ. The quasielastic broadening is small but significant.

V. RESULTS

A. Elementary jump

Two types of jumps for Ni atoms into vacant sites of the $B2$ phase of NiGa are possible: NNN jumps between sites of the Ni sublattice and NN jumps to and from antistructure sites.

Figure 4 shows the linewidths Γ of single Lorentzians extracted from the experimental spectra compared to the linewidths calculated on the basis of the NNN-jump model, Eq. (1). The agreement between the calculated and experimental linewidths is not satisfactory, especially at high values of Q where $S(\mathbf{Q},\omega)$ is sensitive to the dynamics on the atomic scale.

For the NN jumps the data analysis is more subtle: Given the small contribution of the broad Lorentzian a two-line fit in single-experimental spectra cannot yield more than the order of magnitude of the linewidth of the broad Lorentzian. Therefore we proceeded in the following way: instead of fitting two lines to every spectrum separately we calculate the weights and widths of the two Lorentzians *for all single-crystal orientations and scattering angles* belonging to one temperature *simultaneously* as a function of β and D_{Ni}. This means that instead of two parameters for each spectrum (the widths Γ of the two independent lines) there are only two parameters (D_{Ni} and β) for the 6 or 18 spectra at each temperature which strongly increases the reliability of the results. The fitting procedure was performed using the program AGATHE[18]. The agreement with the experimental data is best at high Q values, which are connected to the diffusion process on the atomistic scale. Small deviations at $Q=0.52$ Å^{-1} might be explained by a contribution of multiple scattering as the spectra with smaller line broadening are more sensitive to this effect. Since the shape of the lines is less sensitive to β than to D_{Ni}, an exact determination of β was only possible for temperatures and concentrations with three different orientations, i.e., 18 spectra. Table III shows the values of β obtained by the fit.

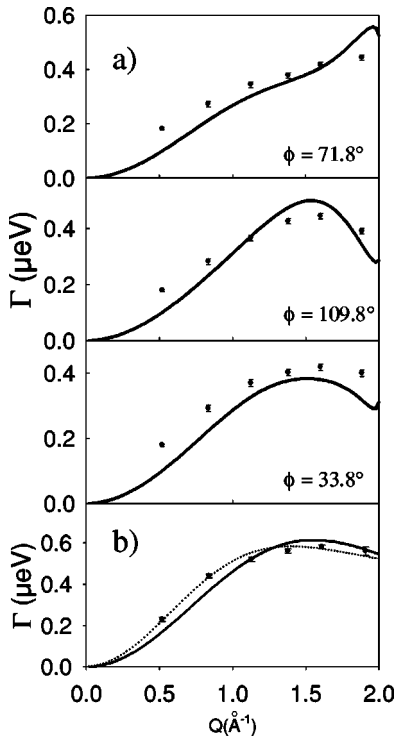

FIG. 4. (a) Points: FWHM of Lorentzians fitted into the quasielastic spectra of $Ni_{51.2}Ga_{48.8}$ at 1130 °C. Lines: Linewidths calculated on the basis of the NNN-jump model. The three different plots represent three different orientations ϕ of the single crystal. (b) Points: FWHM of Lorentzians fitted into the quasielastic spectra of polycrystalline $Ni_{61.9}Ga_{38.1}$ at 1150 °C. Lines: linewidths calculated on the basis of NNN jumps (solid line) and NN jumps using the effective-jump model (dotted line) with $P_{\langle 100\rangle}/P_{\langle 110\rangle}=2.7$.

Unfortunately it is not possible to compare the linewidths of the NN model directly to those of the NNN model given in Fig. 3, because the numbers of Lorentzians predicted by the two models are different. To compare the two models we use the deviation of the theoretical curves, $S(\mathbf{Q},\omega)_{th}$, from the experimental spectra, $S(\mathbf{Q},\omega)_{expt}$, expressed in terms of a χ^2 expression. One has to be aware that the physically interesting quantity obtained in the experiment is the scattering function $S(\mathbf{Q},\omega)$, and not the count rate, which is normalized by the incident flux per channel. For this reason we do not use the common definition of χ^2 in terms of counts per channel but

TABLE III. Diffusion constants and vacancy concentrations.

Sample	Single crystal	T(°C)	β	c_V	$D_{Ni}(10^{-12}$ m^2/s)
51.2 at. % Ni	Yes	990	-	-	1.12(20)
51.2 at. % Ni	Yes	1060	-	-	2.31(40)
51.2 at. % Ni	Yes	1130	0.118	0.084	5.12(50)
52.5 at. % Ni	Yes	1060	0.077	0.026	2.32(40)
57.2 at. % Ni	No	1130	-	-	5.44(80)
61.9 at. % Ni	No	1040	-	-	3.14(80)
61.9 at. % Ni	No	1150	-	-	7.42(50)

$$\chi^2 = \sum_{\text{channels}} \frac{[S(\mathbf{Q},\omega)_{th} - S(\mathbf{Q},\omega)_{expt}]^2}{S(\mathbf{Q},\omega)_{th}}. \quad (9)$$

The $S(\mathbf{Q},\omega)_{th}$ are calculated according to Eq. (1) for NNN jumps and Eqs. (4) and (5) for NN jumps. The free parameters in those models were refined using AGATHE as described above. The comparison of the χ^2 values for the NNN and the NN model in Fig. 5 shows that the NN-jump model gives a much better fit to the experimental data.

While Mössbauer experiments[3] showed that the iron atoms in FeAl prefer combinations of NN jumps that lead to effective jumps along the $\langle 110\rangle$ axis, no such preference could be found in the present case. On the contrary, when applying the effective-jump approximation, Eq. (7), our fits show a preference of the nickel atoms for $\langle 100\rangle$ jumps. For example, at 51.2 at. % Ni and 1130 °C we find roughly the following ratio of probabilities for effective jumps: $P_{\langle 100\rangle}:P_{\langle 110\rangle}:P_{\langle 111\rangle}=4:2:1$, while this ratio is expected to be 3:3:1 for an uncorrelated process. However, this result should not be overestimated since the effective-jump model assumes the residence time on the antistructure site to be zero—an approximation which is less suitable for NiGa than for FeAl,[3] where the residence time on the antistructure site is considerably smaller.

An interesting point is that both the NN model, Eqs. (4)–(6), and the effective jump approximation indicate the presence of effective $\langle 111\rangle$ jumps, a combination of NN jumps that does not occur in the six-jump cycle. The contribution of effective $\langle 111\rangle$ jumps is about one-seventh of the total of effective jumps.

B. Defect concentrations

According to Eq. (3) the ratio β of the residence times is directly related to the concentration of Ni antistructure atoms. Under the assumption that the predominating defect type is the triple defect,[19,20] that is to say, that Ni antistructure atoms and vacancies on the Ni sublattice are the only allowed defects, we get vacancy concentrations c_V (referred to the number of atoms) of 2.6(1.0)% at 52.5 at. % Ni and 1060°C and 8.4(1.0)% at 51.2 at. % Ni and 1130°C.

Using the model of Neumann, Chang, and Lee[21] it is furthermore possible to derive the vacancy concentration at stoichiometric composition, the disorder parameter α. By doing so, we obtain $\alpha=0.037(20)$ at 990 °C and $\alpha=0.091(20)$ at 1130 °C. These results are in agreement with the extrapolation of the values obtained by Ho *et al.*[22] and Van Ommen,[23] both using dilatometric methods.

C. Composition far off stoichiometry

The quasielastic spectra of the polycrystalline sample at 61.9 at. % Ni were refined with the polycrystalline approximation, Eq. (8). Here, again, a fit with a NNN model leads to an unsatisfying result (Fig. 4). Unfortunately it is impossible to get an analytical closed-form powder-average expression for the NN model, which assumes jumps between sites of a

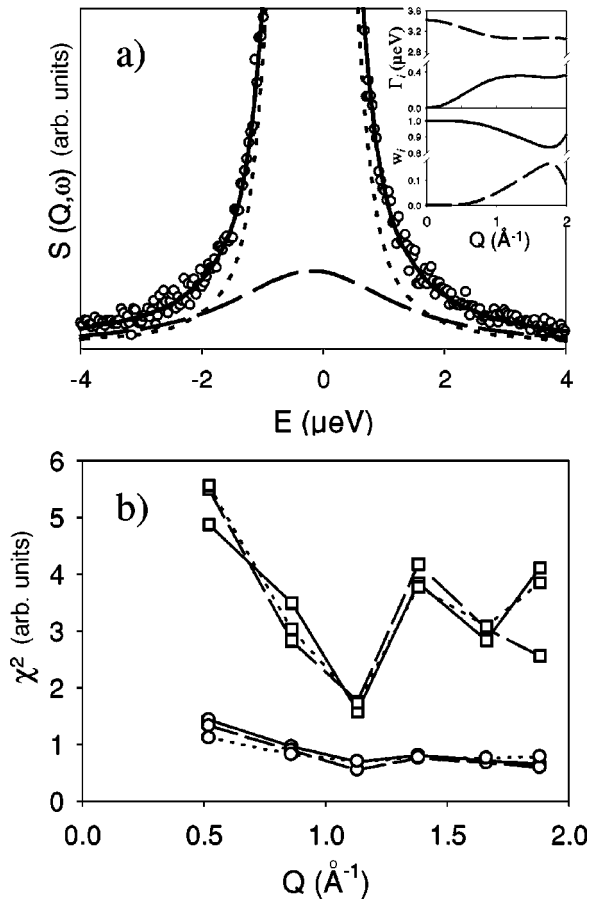

FIG. 5. (a) Quasielastic spectrum ($T=1130$ °C, $Q=1.6$ Å^{-1}, and $\phi=33.8°$) fitted with the sum (solid line) of a narrow (dotted line) and a broad (dashed line) Lorentzian. Inset: FWHM Γ_i in μeV and relative weights w_i for the two Lorentzians as calculated on the basis of NN jumps for $\phi=33.8°$ and $\beta=0.118$. (b) Deviation of spectra fitted according to the NNN jump (squares) and the NN-jump model (circles) from the experimental scattering function $S(\mathbf{Q},\omega)$ as described by Eq. (9). Note that the scale for χ^2 is arbitrary as the sum is performed over $S(\mathbf{Q},\omega)$ and not over the count rate. χ^2 is obtained from fits for three orientations at 1130 °C. Solid line: $\phi=71.8°$. Dashed line: $\phi=109.8°$. Dotted line: $\phi=33.8°$.

non-Bravais lattice. However, a good agreement can be achieved by combining the polycrystalline approximation with the effective-jump approximation, Eq. (7), which assumes NN jumps. Like for the near-stoichiometric compositions, there are indications for a preference of effective $\langle 100 \rangle$ jumps over effective $\langle 110 \rangle$ jumps. Hence, no concentration dependence of the elementary jump vector can be observed on the Ni-rich side of the $B2$ phase of NiGa.

D. Diffusion constants

QNS experiments not only permit one to determine the diffusion process on an atomistic scale, but they also allow one to determine the diffusion constant of the scattering atoms. Two conditions have to be fulfilled.

(a) The length of the atomic jump vector $\mathbf{l}$ has to be known. For jumps between nearest-neighbor sites, $|\mathbf{l}|$ equals $\sqrt{3}/2$ times the lattice constant.

(b) It has to be sure that every atomic jump contributes to the long-range diffusion. An advantage of QNS over QMS is that with QNS this can be verified directly by comparing the linewidths at large values of $Q(>1\ \text{Å}^{-1})$ with the linewidths at small Q which are connected to long-range diffusion. In the present study the observed line broadenings at small momentum transfers are compatible with those at high Q values. Therefore, we conclude that the observed atomistic diffusion mechanism is effective for long-range diffusion.

The diffusion constant is a function of the fitted model parameters τ_{Ga}^{-1} and β:

$$D_{Ni} = \frac{a^2 \beta}{4 \tau_{Ga}(\beta+1)}, \tag{10}$$

where a denotes the lattice constant. The diffusion constants for Ni as measured in the experiment can be found in Table III. Obviously, the concentration dependence of the Ni diffusivity remains weak up to the boundary on the Ni-rich side of the $B2$ phase. A comparison with the diffusion constants obtained by Donaldson and Rawlings[7] at near-stoichiometric composition is given in Fig. 6. Although the two measurements yield the same temperature dependence of D_{Ni}, the absolute values obtained by QNS are somewhat higher than those from the tracer measurements. As the QNS experiment is performed *in situ*, the only source of error can be the measurement of the temperature. Because of the large homogeneous zone of the furnace, the latter can be regarded as trustworthy, which incites us to trust the values from the QNS experiment. From the slope of the temperature dependence of D_{Ni} in the Arrhenius plot an activation energy of 1.66(20) eV near stoichiometry is derived in agreement with the values of Donaldson and Rawlings[7]. For the off-stoichiometric composition with 61.9 at. % Ni we obtain an activation energy of 1.26(20) eV.

VI. DIFFUSION MECHANISM

The QNS measurement clearly shows that nickel atoms in NiGa diffuse via antistructure sites. With this mechanism a problem concerning the local order is associated. Several models have been proposed in order to overcome this problem: the antistructure-bridge mechanism (ASB), the triple-defect mechanism (TDM), and the six-jump cycle (6JC).

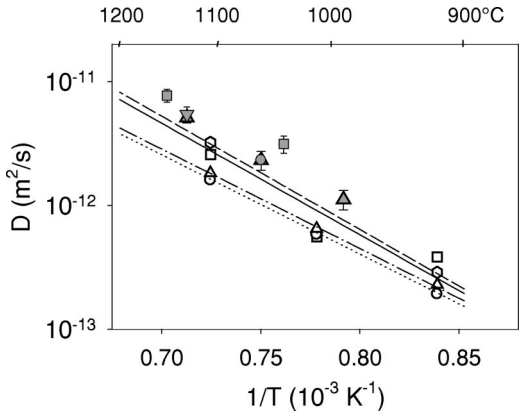

FIG. 6. Arrhenius plot of Ni Diffusion constants in NiGa near stoichiometry. Solid symbols: this work at 51.2 at. % Ni (triangles up), 52.5 at. % Ni (circle), 57.2 at. % Ni (triangle down) and 61.9 at. % Ni (squares). Open symbols and lines: Donaldson and Rawlings, 50 at. % Ni (squares and solid line), 50.5 at. % Ni (hexagons and dashed line), 51 at. % Ni (circles and dotted line) and 52.4 at. % Ni (triangles and dashed-dotted line). Note that two points are overlapping at 1060 and 1130°C, respectively.

These mechanisms shall be discussed in the following with regard to the results of the QNS experiments.

(a) ASB: Belova and Murch[24] showed on the basis of Monte Carlo simulations that the ASB mechanism cannot be effective for long-range diffusion at stoichiometric composition as long as the concentration of antistructure atoms is smaller than 0.14 which is much more than the values obtained in this study for the near stoichiometric compositions. For the sake of completeness we would like to mention that a quasielastic broadening observed in the QNS experiment could in principal originate in forward and backward jumps of atoms on nonpercolating ''ASB islands.'' However, if this were the case, an anomalous small line broadening at the small values of $\mathbf{Q}$ where QNS is sensitive to long-range diffusion would be expected. From the fact that such an effect has not been observed and that the diffusion constants measured in the QNS experiment are—within the experimental errors—in agreement with those obtained from the tracer experiments, we conclude that another mechanism than the ASB has to be operative even on the atomistic scale.

(b) TDM: The TDM has been proposed by Stolwijk *et al.*[9] in order to explain the results of tracer diffusion experiments on CoGa. In this model the A atom (Co in CoGa, Ni in NiGa) performs NN jumps profiting of double vacancies. The state with the A atom on the antistructure site next to two vacancies on the A sublattice is considered to be the stable state. The Ga atoms on the B sublattice are considered to jump between the unit cells by NNN jumps, i.e., from one B site to the next. While this mechanism can be supported by our results, as far as the motion of the nickel atoms is concerned, there is some inconsistency concerning the activation energies of nickel and gallium diffusion: The activation energies that are attributed to the TDM by Stolwijk *et al.*[9] are the same for Co and Ga diffusion since the diffusion of Co and Ga is strongly coupled. On the other hand, Ref. 7 finds very different activation energies for Ni and Ga atoms which indicates a less coupled diffusion mechanism for the two components. Hence, a pure TDM as found in CoGa cannot be operative in NiGa.

(c) 6JC: Monte Carlo simulations[25] showed that the ratio of effective jumps, $P_{\langle 110\rangle}/P_{\langle 100\rangle}=1.7$, found in FeAl with QMS,[3] is compatible with a diffusion mechanism based on the 6JC, even though this ratio is not within the limits given by Arita *et al.*[26] Recently, it has been shown analytically[27] that every ratio $P_{\langle 110\rangle}/P_{\langle 100\rangle}$ is allowed for the 6JC if one drops some restrictive assumptions. However, even then the 6JC cannot account for the contribution of $\langle 111\rangle$ jumps in NiGa, which has been found in the QNS experiment. Hence, the 6JC cannot apply for the diffusion in NiGa at high temperatures, at least not exclusively.

In our opinion, the reason for the fact that none of the models cited above is able to explain the experimental data can be found in the high defect concentrations. It is difficult to argue that a single vacancy should, e.g., carry out a whole six-jump cycle when another defect in the neighborhood is able to restore local order without requiring further energetically expensive jumps. If one considers also the high concentrations of antistructure atoms and vacancies, there are various cycles imaginable that include two or more defects and that reduce considerably the number of wrong bonds compared to the six-jump cycle. In addition, as has been pointed out by Kiguchi and Sato,[28] it is not absolutely necessary that the local order is restored after each unit process at such high defect concentrations as long as the degree of order over the whole sample is conserved.

VII. SUMMARY

Quasielastic neutron scattering allowed us to confirm the very weak concentration dependence of the Ni diffusivity in NiGa, observed by Donaldson and Rawlings[7] with tracer diffusion around stoichiometry, over a wide concentration range on the Ni rich side of the $B2$ phase of NiGa. However, the next-nearest-neighbor jumps of Ni that have been proposed by Donaldson and Rawlings to explain their data could not be found. On the contrary, the QNS experiment showed that the Ni atoms diffuse via *nearest-neighbor jumps* to antistructure sites—despite the high enthalpy of formation of NiGa.

The residence time of the Ni atom on the Ga sublattice has been found to be about 0.08 and 0.12 times the residence time on the Ni sublattice at 1060 and 1130 °C for the near-stoichiometric compositions. From this, very high concentrations of antistructure atoms and vacancies are derived.

The fact that none of the common models for diffusion in terms of closed cycles is able to explain consistently the QNS *and* the tracer diffusion data can be seen as a consequence of these high defect concentrations.

ACKNOWLEDGMENTS

We would like to thank M. Hartmann for help with the sample preparation. This work was supported by grants from the Austrian FWF (Project Nos. S5601 and P10739-CHE).

[1] H. Mehrer, Mater. Trans., JIM **37**, 1259 (1996).
[2] M. Koiwa, in *Ordered Intermetallics—Physical Metallurgy and Mechanical Behaviour*, edited by C. T. Liu *et al.* (Kluwer, Dordrecht, 1992), p. 449.
[3] G. Vogl and B. Sepiol, Acta Metall. Mater. **42**, 3175 (1994).
[4] B. Sepiol, C. Czihak, A. Meyer, G. Vogl, J. Metge, and R. Rüffer, Hyperfine Interact. **113**, 449 (1998).
[5] Y. Mishin and D. Farkas, Defect Diffus. Forum **143-147**, 303 (1997); Y. Mishin and D. Farkas, Scr. Mater. **39**, 625 (1998).
[6] J. P. Neumann, Acta Metall. **28**, 1165 (1980).
[7] A. T. Donaldson and R. D. Rawlings, Acta Metall. **24**, 285 (1976).
[8] J. P. Neumann, Y. A. Chang, and H. Ipser, Scr. Metall. **10**, 917 (1976).
[9] N. A. Stolwijk, M. van Gend, and H. Bakker, Philos. Mag. A **42**, 783 (1980).
[10] P. Feschotte and P. Eggimann, J. Less-Common Met. **63**, 15 (1974).
[11] G. Vogl, O. G. Randl, W. Petry, and J. Hünecke, J. Phys.: Condens. Matter **5**, 7215 (1993).
[12] G. Vogl, M. Kaisermayr, and O. G. Randl, J. Phys.: Condens. Matter **8**, 4727 (1996).
[13] M. Kaisermayr, J. Combet, B. Sepiol, H. Thiess, and G. Vogl, Physica B **270**, 276 (2000).
[14] C. T. Chudley and R. J. Elliott, Proc. Phys. Soc. London **77**, 353 (1961).
[15] O. G. Randl, B. Sepiol, G. Vogl, R. Feldwisch, and K. Schroeder, Phys. Rev. B **49**, 8768 (1994).
[16] H. Ipser, A. Mikula, and W. Schuster, Monatsch. Chem. **120**, 283 (1989).
[17] V. F. Sears (unpublished).
[18] M. Bée (unpublished).
[19] R. J. Wasilewski, S. R. Butler, and J. E. Hanlon, J. Appl. Phys. **39**, 4234 (1968); R. J. Wasilewski, J. Phys. Chem. Solids **29**, 51 (1968).
[20] Y. A. Chang and J. P. Neumann, Prog. Solid State Chem. **14**, 221 (1982).
[21] J. P. Neumann, Y. A. Chang, and C. M. Lee, Acta Metall. **24**, 593 (1976).
[22] K. Ho, M. A. Quader, F. Lin, and R. A. Dodd, Scr. Metall. **11**, 1159 (1977).
[23] A. H. Van Ommen, Phys. Status Solidi B **72**, 273 (1982).
[24] I. V. Belova and G. E. Murch, Intermetallics **6**, 119 (1998).
[25] R. Weinkamer, P. Fratzl, B. Sepiol, and G. Vogl, Phys. Rev. B **59**, 8622 (1999).
[26] M. Arita, M. Koiwa, and S. Ishioka, Acta Metall. **37**, 1363 (1989).
[27] R. Drautz and M. Fähnle, Acta. Mater. **47**, 2437 (1999).
[28] R. Kiguchi and H. Sato, J. Chem. Phys. **51**, 161 (1969).